under near-equilibrium as well as far-from-equilibrium conditions.

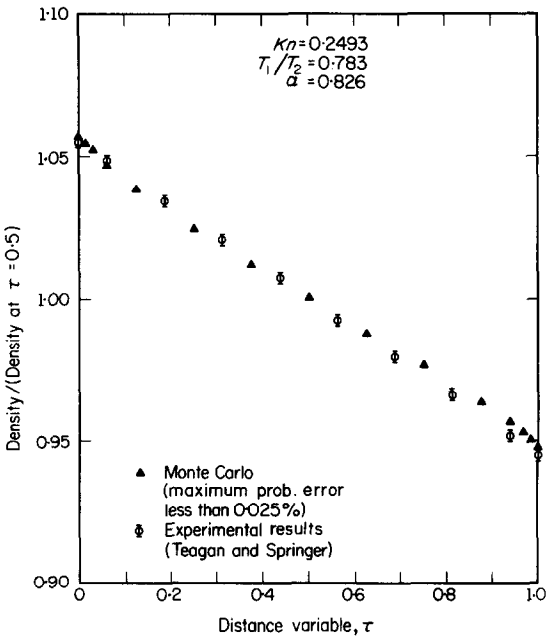

FIG. 6. Comparison of a density profile with that determined in an experiment.

ACKNOWLEDGEMENT

This work was supported by the Joint Services Electronics Program (Contract Army DAAB-07-67-C-0199) and the Office of Naval Research (contract N00014-67-A-0305-0001).

REFERENCES

1. A. NORDSIEK and B. L. HICKS, Monte Carlo evaluation of the Boltzmann collision integrals, Proc. Fifth Intl. Symp on Rar. Gas Dyn., Vol. 1, pp. 695–710 (1967).
2. S. M. YEN and H. J. SCHMIDT, Monte Carlo solutions of the Boltzmann equation for heat transfer problems, Proc. Sixth Intl. Symp. on Rar. Gas Dyn., Vol. 1, pp. 205–213 (1969).
3. S. M. YEN, Solutions of the Boltzmann and Krook equations for heat transfer problems with Maxwell boundary conditions, Proc. Seventh Intl. Symp. on Rar. Gas Dyn. (to be published).
4. D. G. ANDERSON and H. K. MACOMBER, Numerical experiments in kinetic theory, Proc. Fourth Intl. Symp. on Rar. Gas Dyn., Vol. 1, pp. 96–111 (1965).
5. M. LAVIN, A Monte Carlo solution for heat transfer in rarefied gases, M.S. Thesis, MIT (1961).
6. J. K. HAVILAND, The solution of two molecular flow problems by the Monte Carlo method, *Meth. Comp. Phys.* **4**, 109–209 (1965).
7. M. PERMUTTER, Analysis of Couette flow and heat transfer between two parallel plates enclosing rarefied gas by Monte Carlo, Proc. Fifth Symp. on Rar. Gas Dyn., Vol. 1, pp. 455–480 (1967).
8. W. P. TEAGEN and C. P. SPRINGER, Heat transfer and density distribution measurements between parallel plates in the transition regime, *Physics Fluids* **11**, 497–506 (1968).

Int. J. Heat Mass Transfer. Vol. 14, pp. 1869–1873. Pergamon Press 1971. Printed in Great Britain

MASS TRANSFER DURING FILM BOILING ON VERTICAL FIBERS

VERNON A. NIEBERLEIN

Physical Sciences Directorate, Research, Development, Engineering and Missile Systems Laboratory, U.S. Army Missile Command, Redstone Arsenal, Alabama 35809, U.S.A.

(*Received* 22 *December* 1970 *and in revised form* 10 *May* 1971)

NOMENCLATURE

A, fiber cross-sectional area [cm^2];
A_s, final fiber cross-sectional area [cm^2];
A_w, tungsten wire cross-sectional area [cm^2];
D, mass diffusivity [cm^2 min^{-1}];
D_{av}, average diameter of the deposit [cm];
D_s, diameter of the deposit [cm];
D_w, diameter of the tungsten wire [cm];
f, a function defined by equation (10) [cm^{-1}];
g, gravitational constant [cm min^{-2}];
h, thickness of a fiber slice [cm];
k_z, rate constant [g moles cm^{-2} min^{-1} in.$^{0.246}$];
E, liquid evaporation rate [cm min^{-1}];
M_s, molecular weight of SiC;

m, exponent of voltage [dimensionless];
n, exponent of mass fraction [dimensionless];
n_A, mass flux of component A [g cm^{-2} min^{-1}];
N_{Sc}, Schmidt number [dimensionless];
P, proportionality constant [g moles cm^{-2} min^{-1} V^{-m}];
p, proportionality constant [g moles cm^{-2} min^{-1}];
q, exponent of vertical distance [dimensionless];
r, radius [cm];
r_i, radius of the substrate [cm];
R, deposition rate of SiC [g moles cm^{-2} min^{-1}];
V, applied potential [V];
v_r, radial velocity [cm min^{-1}];
v_z, vertical velocity [cm min^{-1}];
z, vertical distance [cm];
δ, radius of the gas envelope [cm];
ζ, dimensionless stream function;
η, dimensionless radius;
η_δ, dimensionless radius of the liquid–vapor interface;
η_i, dimensionless radius at the fiber wall;
θ, angular coordinate [radians];
μ, viscosity [g cm^{-1} min^{-1}];
ρ_s, density of SiC [g cm^{-3}];
ρ_L, density of the liquid [g cm^{-3}];
ρ_V, density of the vapor [g cm^{-3}];
ψ, stream function [cm^3 min^{-1}];
ω_A, mass fraction of component A [dimensionless];
ω_{A_i}, mass fraction of component A at the wall [dimensionless];
ω_{A_δ}, mass fraction of component A at the liquid–vapor interface [dimensionless];
Ω_A, proportional mass fraction of A [dimensionless].

1. INTRODUCTION

HIGH-MODULUS fibers for aerospace applications have been prepared by a variety of methods, depending upon the material. One of the most important of these methods is chemical vapor deposition [1–5], whereby a hot filament is pulled through a chamber filled with a gaseous reactant which deposits a coating on the wire. Free or forced convection brings up fresh reactant. It has recently been shown that such fibers can also be prepared by mass transport during film boiling [6], providing the reactants are liquids, and the vapors from the liquids pyrolyze or otherwise react to give the required deposit. The liquid reactant used in this investigation was $(CH_3)_3SiCl$ in cyclohexane, which pyrolyzes to give SiC.

Deposition of SiC from $(CH_3)_3SiCl$ is well known [7–9], but this has always been accomplished without film boiling. Exploratory experiments showed that submersion of the hot surface into the liquid reactant would indeed result in a silicon carbide deposit comparable to that obtained from forced convection of the vapor. The liquid technique carried some advantages in simplicity, plating rate, and size of equipment. The object of the present research, therefore, was to understand the mechanisms involved, in order to make the film boiling process more useful.

2. THEORETICAL ANALYSIS

Heat transfer during film boiling has been analyzed by a number of investigators [10–16], and mass transfer appears analogous. The system geometry dictated a cylindrical model with the submerged vertical fiber surrounded by a parabolic gas envelope of variable radius δ. The equations for continuity, momentum, and continuity of $(CH_3)_3SiCl$ (designated as component A), are given below with the following assumptions.

1. The process is diffusion controlled.
2. The gas flow is laminar.
3. Steady-state conditions apply.
4. Fluid properties are constant.
5. There is no angular dependence (θ-direction) of any variable.
6. Effective momentum and mass transfer by diffusion takes place in the r-direction only.
7. There are no homogeneous gas-phase chemical reactions.
8. The radius of the substrate is insignificantly small.

$$\text{Continuity: } \frac{1}{r}\frac{\partial}{\partial r}(rv_r) + \frac{\partial v_z}{\partial z} = 0. \tag{1}$$

$$\text{Motion: } v_r\frac{\partial v_z}{\partial r} + v_z\frac{\partial v_z}{\partial z} = \frac{\mu}{\rho_v}\frac{1}{r}\frac{\partial}{\partial r}\left(r\frac{\partial v_z}{\partial r}\right) + \frac{\rho_L - \rho_V}{\rho_V}g. \tag{2}$$

$$\text{Continuity of } A: v_r\frac{\partial \omega_A}{\partial r} + v_z\frac{\partial \omega_A}{\partial z} = D\frac{1}{r}\frac{\partial}{\partial r}\left(r\frac{\partial \omega_A}{\partial r}\right). \tag{3}$$

These equations carry the following boundary conditions.

$$\text{At } r = r_i: \quad v_r = v_z = 0 \quad \omega_A = 0. \tag{4}$$

$$\text{At } r = \delta: \quad v_z = 0 \quad \omega_A = \omega_{A_\delta} \quad \frac{\partial \omega_A}{\partial r} = \frac{\omega_{A_\delta}}{D}\left(\frac{\rho_L}{\rho_V}E + v_r\right). \tag{5}$$

where E is the liquid evaporation rate.

The stream function ψ is introduced and is defined as follows.

$$v_z = -\frac{1}{r}\frac{\partial \psi}{\partial r} \quad \text{and} \quad v_r = \frac{1}{r}\frac{\partial \psi}{\partial z}. \tag{6}$$

Substitution of (6) into (1) satisfies equation (1). Substitution of (6) into (2) and (3) results in the following.

$$-\frac{1}{r^2}\frac{\partial \psi}{\partial z}\frac{\partial^2 \psi}{\partial r^2} + \frac{1}{r^3}\frac{\partial \psi}{\partial z}\frac{\partial \psi}{\partial r} + \frac{1}{r^2}\frac{\partial \psi}{\partial r}\frac{\partial^2 \psi}{\partial r \partial z} = -\frac{\mu}{\rho_V}\frac{1}{r}\frac{\partial^3 \psi}{\partial r^3} + \frac{\mu}{\rho_V}\frac{1}{r^2}\frac{\partial^2 \psi}{\partial r^2} - \frac{\mu}{\rho_V}\frac{1}{r^3}\frac{\partial \psi}{\partial r} + \frac{\rho_L - \rho_V}{\rho_V}g \tag{7}$$

$$\frac{\partial\psi}{\partial z}\frac{\partial\omega_A}{\partial r} - \frac{\partial\psi}{\partial r}\frac{\partial\omega_A}{\partial z} = \frac{\mu}{\rho_V N_{Sc}}\left(r\frac{\partial^2\omega_A}{\partial r^2} + \frac{\partial\omega_A}{\partial r}\right). \quad (8)$$

To transform (7) and (8) into a set of ordinary differential equations, the following changes of variables are made.

$$\eta = fr \quad (9)$$

$$f = \left[\frac{\rho_V(\rho_L - \rho_V)g}{4\mu^2}\right]^{\frac{1}{4}} z^{-\frac{1}{4}}. \quad (10)$$

$$\psi = \frac{4\mu}{\rho_V} z\zeta \quad (11)$$

$$\Omega_A = \frac{\omega_A - \omega_{A_\delta}}{\omega_{A_i} - \omega_{A_\delta}}. \quad (12)$$

Introducing (9)–(12) into (7) and (8) results in equations (13) and (14) respectively, where primes indicate differentiation with respect to η.

$$\zeta''' - \frac{1}{\eta}\zeta'' - \frac{4}{\eta}\zeta\zeta'' + \frac{4}{\eta^2}\zeta\zeta' + \frac{2}{\eta}(\zeta')^2 + \frac{1}{\eta^2}\zeta' - \eta = 0 \quad (13)$$

$$\Omega_A'' + \left(\frac{1}{\eta} - 4N_{Sc}\frac{\zeta}{\eta}\right)\Omega_A' = 0. \quad (14)$$

The boundary conditions transform to the following.

$$\text{At } \eta = \eta_i\text{:}\quad \zeta = \zeta' = 0 \quad \Omega_A = 1 \quad (15)$$

$$\text{At } \eta = \eta_\delta\text{:}\quad \zeta' = 0$$

$$\Omega_A = 0 \quad \frac{d\Omega_A}{d\eta} = -\frac{N_{Sc}}{\mu}\left(\frac{\rho_L}{f}E + \frac{4\mu}{\eta_\delta}\zeta\right). \quad (16)$$

Equations (13) and (14) may be solved if there is an interest in the velocity profile and mass fraction profile of A in the gas envelope. However, for the purpose of determining the mass flux of A, equations (9), (10) and (12) which are used to make the transformation, are needed and used below.

The mass flux of A (trimethylchlorosilane) in the r-direction is given by

$$n_A = -\rho_V D\frac{\partial\omega_A}{\partial r} + \omega_A(n_A + n_B + n_C + \ldots). \quad (17)$$

The reaction at the wall is irreversible and diffusion limited, so that

$$\omega_{A_i} = 0. \quad (18)$$

Therefore, at the wall (17) becomes

$$n_A\big|_{r=r_i} = -\rho_V D\left.\frac{\partial\omega_A}{\partial r}\right|_{r=r_i}. \quad (19)$$

Substituting (18) into (12), differentiating, and using equation (9),

$$\frac{d\omega_A}{dr} = -\omega_{A_\delta}\frac{d\Omega_A}{dr} = -\omega_{A_\delta} f\frac{d\Omega_A}{d\eta}. \quad (20)$$

Introducing (10) into (20) and then (20) into (19) results in

$$n_A\Big|_{\eta=\eta_i} = \rho_V D\left[\frac{\rho_V(\rho_L - \rho_V)g}{4\mu^2}\right]^{\frac{1}{4}}\left(\frac{\omega_{A_\delta}}{z^{\frac{1}{4}}}\right)\left.\frac{d\Omega_A}{d\eta}\right|_{\eta=\eta_i}. \quad (21)$$

Equation (21) states that the mass flux of trimethylchlorosilane at the fiber wall is directly proportional to the mass fraction of trimethylchlorosilane at the vapor–liquid interface and inversely proportional to the one-fourth power of the distance up the fiber. An experimental program was undertaken to verify this.

3. EXPERIMENTAL PROCEDURE

A plating cell was constructed which consisted of a one-inch diameter vertical quartz tube surrounded by a water jacket and a metal closure at each end. Two-mil tungsten wire entered the top, passed over guide pegs, a platinum contact peg, then out through a mercury well at the bottom. Resistive heating was accomplished by d.c. applied between the platinum peg and the mercury well, a distance of 2 in. Voltages used were 18·0–20·0 in increments of 0·5 V. This resulted in temperatures in the neighborhood of 880°C, but control was by voltage alone because of the unreliability associated with optical pyrometry through a colored solution, and a rapidly varying temperature. The increasing thickness of the conductive coating precluded the use of the fiber itself as a resistance thermometer. The solutions used were 10, 20, 30, 40, 70 and 100 liquid volume per cent of $(CH_3)_3SiCl$ in C_6H_{12} (cyclohexane), and all plating was for a duration of 2 min.

An "aging" period was required on each solution before measurements could be taken. New solutions produced deposits of low electrical conductivity, but as the plating proceeded the conductivity increased. This variable caused the fiber temperature and deposition rate to change for the first 5–10 min of solution use. After the initial colorless solution changed to amber from the accumulation of by-products, the deposition rate became constant, and remained so, for at least 1 h of plating time. Thus, to obtain greater confidence of accuracy, all runs were made in duplicate, following an initial 20-min period of plating at 19·0 V. The first of the duplicate series was made using ascending voltages, starting at 18·0 V. The second was made in a different solution using descending voltages starting at 20·0 V. Averaging cancelled any effect of solution depletion while the experiment was in progress. Actually no real trend was noted that could be attributed to solution depletion.

After plating, the fibers were mounted in a fixture for microscopic examination. A micrometer mounted on the stage permitted any station on the fiber to be located within 0·0005 in., and a measuring scale on the eyepiece permitted the diameter to read to within 2 μ. Measurements were made at 16 stations along the fiber.

Deposition rates were calculated as follows. A slice of fiber, of thickness dh, includes an annular SiC deposit of density ρ_s, and external and internal diameters D_s and D_w respectively. Since deposition takes place on the edge of this slice only, and over a 2-min interval, the rate of deposition is

$$R = \frac{\pi(D_s^2 - D_w^2)\,dh\,\rho_s}{8(\pi D_{av}\,dh)\,M_s}, \tag{22}$$

where M_s is the molecular weight of SiC D_{av} is related to the instantaneous cross-sectional area of the fiber as follows,

$$D_{av} = \frac{\frac{2}{\sqrt{\pi}}\int_{A_w}^{A_s}(\sqrt{A})\,dA}{A_s - A_w} = \frac{2(D_s^3 - D_w^3)}{3(D_s^2 - D_w^2)}, \tag{23}$$

where A_s and A_w are the final fiber cross-sectional area and the tungsten cross-sectional area respectively. Substituting (23) into (22), and using $M_s = 40{\cdot}07$ g mole^{-1}, $\rho_s = 3{\cdot}217$ g cm^{-3}, $D_w = 0{\cdot}005$ cm, the deposition rate in moles cm^{-2} min^{-1} becomes

$$R = \frac{0{\cdot}01505\,(D_s^2 - 0{\cdot}000025)^2}{D_s^3 - 0{\cdot}000000125}. \tag{24}$$

To verify the inverse one-fourth power dependency of rate with vertical distance, as shown by equation (21), a computer program was written to find the best-fit curves of the type

$$R = k_z z^q \tag{25}$$

for the data obtained from the plating experiments. Curves were fit at six $(CH_3)_3SiCl$ concentrations and at five plating voltages. Computed best-fit values for q are given in Table 1.

A standard error of estimate was calculated for each of the thirty curves described by equation (25), using the best-fit value for q given in Table 1. These standard errors of estimate were divided by an average R to get a coefficient of variation. The average R was obtained by dividing the area under each R–z curve by the deposit length. The coefficients of variation are given in Table 2.

In order to investigate the deposition rate as a function of the mass fraction of $(CH_3)_3SiCl$ in the vapor at the liquid–vapor interface it was first necessary to determine these mass fractions experimentally. A distillation apparatus very similar to that constructed by Othmer [17] was built. This equipment allowed no refluxing, and the distillate overflowed from the receiver back into the boiler. Fifty ml of the $(CH_3)_3SiCl$–C_6H_{12} mixture was the normal charge placed in the boiler, and the distillate was sampled at 10-min intervals, until a constant analysis showed that a condition of steady state had been reached by the system. At this time the boiler was also analyzed. The analysis was by refractive index, using an Abbe refractomer held at 25·0°C by water circulated from a constant temperature bath.

Table 1. Least-squares best-fit values for the exponent of z

Liquid volume % of A	Plating voltage 18·0	18·5	19·0	19·5	20·0
10	−0·28	−0·28	−0·26	−0·26	−0·24
20	−0·30	−0·27	−0·26	−0·27	−0·26
30	−0·23	−0·24	−0·25	−0·26	−0·23
40	−0·28	−0·27	−0·27	−0·26	−0·27
70	−0·25	−0·23	−0·19	−0·19	−0·21
100	−0·20	−0·21	−0·23	−0·23	−0·20

Table 2. Coefficients of variation for best-fit deposition curves

Liquid volume % of A	Coefficient of variation, % 18·0 V	18·5 V	19·0 V	19·5 V	20·0 V
10	4·0	4·8	4·9	3·8	3·8
20	3·4	4·2	3·2	1·5	2·4
30	4·6	4·3	3·4	3·3	5·1
40	2·9	2·6	2·5	2·0	2·5
70	4·0	4·9	3·1	4·0	3·6
100	6·0	4·8	4·2	4·0	5·8

To test the linear dependency of deposition rate with the mass fraction of A at the liquid–vapor interface, as indicated by equation (21), the latter was rewritten as

$$R = p\omega_{A_0}^n. \tag{26}$$

However p is a function of temperature, which in turn is a function of voltage. This condition makes R a function of two variables as shown in equation (27),

$$R = PV^m\omega_{A_0}^n, \tag{27}$$

where V is applied voltage. A computer program was written to determine the least-squares best-fit values of P, m and n for the surface described by equation (27).

4. RESULTS AND DISCUSSION

The experimental work coincides very closely with theory on the dependency of mass transport rate with the negative one-fourth power of the distance up the fiber. Least-squares best-fit values for six concentrations of $(CH_3)_3SiCl$, with each concentration at five temperatures, gave an overall mean value of −0·246 for the exponent of the distance up the fiber.

The linear dependency of mass transport rate with mass fraction of $(CH_3)_3SiCl$ at the vapor–liquid interface, as

indicated by equation (21), did not agree as closely with experiment as the relationship of mass transport with vertical distance. The above mentioned 30 experiments gave a transport rate proportional to the 0·70-power of the trimethylchlorosilane equilibrium mass fraction. This discrepancy between theoretical linear dependency and experimental 0·70-power dependency might be attributed to an inaccuracy in assumption No. 7. A mass spectrometer analysis on the by-product gas showed the presence of 103 chemical species, attesting to the complexity of the pyrolysis reactions. It is not known if these reactions are all heterogeneous. It could be suspected that at least some of these are homogeneous reactions taking place somewhere in the gas envelope as component A approaches the fiber wall. Such reactions would, of course, diminish the flux of A.

The R of equation (27) is an integrated average of the mass transport rates between 0·2 and 1·8 in. above the bottom electrical contact on the fiber. Measurements showed the deposition to take place at this average rate at 0·82 in. above the bottom of the fiber. With this information, and the use of equation (25), (27) can be generalized to reflect the effect on deposition rate of vertical position on the fiber. This generalized equation is

$$R = 2{\cdot}13 \times 10^{-8} V^{3{\cdot}29} \omega_{A_s}^{0{\cdot}70} z^{-0{\cdot}246}. \qquad (28)$$

REFERENCES

1. L. C. McCandless, J. C. Withers and L. G. Davies, High modulus-to-density reinforcements for structural composites, AFML-TR-65-265, Wright–Patterson Air Force Base, Ohio (1965).
2. J. C. Withers and J. P. Redmond, Synthesis by vapor deposition of new filament materials, AFML-TR-66-329, Wright–Patterson Air Force Base, Ohio (1966).
3. L. C. McCandless, R. D. Bajefsky, C. R. Brummett, L. G. Davies, J. P. Redmond, R. G. Shaver and J. C. Withers, High modulus-to-density reinforcements for structural composites, AFML-TR-65-265, Part II, Wright–Patterson Air Force Base, Ohio (1966).
4. J. H. Oxley, High-modulus, high-strength filaments and composites thereof, AFML-TR-65-399, Wright–Patterson Air Force Base, Ohio (1965).
5. J. H. Oxley, High-modulus, high strength filaments and composites, AFML-TR-66-200, Wright–Patterson Air Force Base, Ohio (1966).
6. V. A. Nieberlein, Deposition of silicon carbide from liquid compounds, *SAMPE Jl* **4**(6), 72–74 (1968).
7. S. Susman, R. S. Spriggs and H. S. Weber, Vapor phase growth of β-silicon carbide single crystals, *Silicon Carbide—A High Temperature Semi-Conductor*, J. R. O'Connor and J. Smiltens, pp. 94–109. Symposium Publications Division, Pergamon Press, New York (1959).
8. R. L. Hough and D. E. Early, Silicon carbide from pyrolysis of nonstoichiometric organosilanes, AFML-TR-66-174, Wright–Patterson Air Force Base, Ohio (1966).
9. H. W. Huggins and C. H. Pitt, Characteristics of silicon carbide produced by thermal decomposition of trimethylchlorosilane, *Cer. Bull.* **46**(3), 266–269 (1967).
10. L. A. Bromley, N. R. LeRoy and J. A. Robbers, Heat transfer in forced convection film boiling, *Ind. Engng Chem.—Engng Proc. Dev.* **45**, 2639–2646 (1953).
11. P. W. McFadden and R. J. Grosh, High-flux heat transfer studies: An analytical investigation of laminar film boiling, ANL-6060, Argonne National Lab., Lemont, Ill. (1959).
12. E. M. Sparrow and R. D. Cess, The effect of subcooled liquid on laminar film boiling, *J. Heat Transfer* **84**, 149–155 (1962).
13. K. Nishikawa and T. Ito, Two phase boundary layer treatment of free convection film boiling, *Int. J. Heat Mass Transfer* **9**, 103–115 (1966).
14. L. E. Dean and L. M. Thompson, Study of heat transfer to liquid nitrogen, Am. Soc. Mech. Eng. Paper No. 56-SA-4 (1956).
15. W. F. Laverty and W. M. Rohsenow, Film boiling of saturated nitrogen flowing in a vertical tube, *J. Heat Transfer* **89**, 90–98 (1967).
16. W. H. McAdams, J. N. Addoms, P. M. Rinaldo and R. S. Day, Heat transfer from single horizontal wires to boiling water, *Chem. Engng Prog.* **44**, 639–646 (1948).
17. D. F. Othmer, Composition of vapors from boiling binary solutions, *Ind. Engng Chem.* **20**, 743–746 (1928).